

# Ultrathin Platinum Nanoparticles Encapsulated in a Graphite Lattice—Prepared by a Sonochemical Approach

Jürgen Walter,\* Masato Nishioka, and Shigeta Hara

Department of Materials Science and Processing, Osaka University, 2-1 Yamada-oka, Suita, Osaka 565-0871, Japan

Received November 14, 2000. Revised Manuscript Received March 9, 2001

$\text{H}_2\text{PtCl}_6$  was intercalated into natural graphite by applying ultrasound to a mixture of graphite,  $\text{H}_2\text{PtCl}_6$ ,  $\text{CCl}_4$ , and  $\text{SOCl}_2$  for 3 days. X-ray diffraction data showed that the host lattice was partly intercalated by  $\text{H}_2\text{PtCl}_6$ . A mixture consisting of a third and fourth stage together with unreacted graphite was observed. The intercalation compound was suspended in acetone with hydrogen flowing through while the sonication took place for 2 days. Transmission electron microphotographs showed highly dispersed nanoparticles in a narrow size range inside the carbon lattice. X-ray photoelectron spectroscopy gave evidence that these particles are platinum metal ( $\text{Pt}^0$ ). Particle thickness estimated by X-ray diffraction indicated an average particle thickness of two layers. Selected-area electron diffraction microphotographs showed a pattern that could be hexagonally indexed. A ( $2 \times a_{\text{graphite}}$ ) superstructure was observed for those quasi-two-dimensional aggregates formed by self-organization. This indicates a templating effect due to the carbon lattice.

## Introduction

Noble metals are in use as catalysts for a variety of processes.<sup>1</sup> It is common to disperse the catalytically active metal on an inert substrate, for example, carbon or  $\text{TiO}_2$ . This can be achieved by preparing metal-supported carbons via electrodeposition<sup>1,2</sup> or by mixing carbon and a metal chloride in a solution followed by reduction.<sup>3,4</sup> Metallic nanoparticles will decorate the carbon surface.

Another approach to synthesize metal–carbons is to intercalate a metal chloride in the interlayer space of graphite; for example, see refs 5–7. After reduction by hydrogen gas<sup>8</sup> or by lithium diphenylide,<sup>9,10</sup> it is possible to obtain metallic nanoparticles encapsulated inside the carbon lattice. Depending on the preparation method and metal, metallic monolayers<sup>11</sup> or multilayers<sup>13</sup> produced. This is fundamentally different from Pt-encap-

sulated nanoparticles in polypyrrole films, which are more three-dimensional.<sup>12</sup>

The formation of a graphite intercalation compound (GIC) precursor can be described as a redox reaction. Therefore, the carbon lattice must be oxidized or reduced to introduce guests into the interlayer space of graphite. The driving force for the intercalation reaction is the excess of Coulomb energy. Commonly, graphite and a metal chloride will be mixed together in an ampule and evacuated, and then chlorine gas is added. After the ampule is sealed, the mixture is heated. Another method is to irradiate a mixture of graphite and metal halide in thionyl chloride by short-wave ultraviolet radiation. Because of the irradiation, chlorine radicals will be formed, which are necessary for the redox process.

Graphite intercalation compounds with  $\text{H}_2\text{PtCl}_6$ <sup>14</sup> and Pt nanoparticle inclusions in graphite<sup>1,4,15,16</sup> or Pt-loaded graphite surfaces are known.<sup>15</sup> However, particles generated in the interlayer space by hydrogen gas at high temperatures show Pt nanosheets 5–300-nm wide.<sup>16</sup> Commonly, not all of the graphite reacts. Therefore, Pt contents in graphites with embedded Pt nanoparticles are quite distinguishable. Tilquin et al. found 12.5–21.0 wt % Pt in their samples.<sup>15</sup> Shirai et al.<sup>16</sup> could prepare third-stage intercalation compounds together with unreacted graphite. Their metal content varied strongly: 1–15 wt % Pt; the theoretically available maximum content is 38 wt % Pt.<sup>16</sup>

The contribution of an embedded Pt nanoparticle to electrical conductivity of the sample is very difficult to

\* To whom correspondence should be addressed. Phone + Fax: +81/6/6879-7467. E-mail: walter@mat.eng.osaka-u.ac.jp. URL: <http://surf5.mat.eng.osaka-u.ac.jp/nano>.

(1) Gloaguen, F.; Leger, J. M.; Larny, C. *J. Appl. Electrochem.* **1997**, *27*, 1052.

(2) Lee, I.; Chan, K. Y.; Phillips, D. L. *Ultramicroscopy* **1998**, *75*, 69.

(3) Satishkumar, B. C.; Vogl, E. M.; Govindaraj, A.; Rao, C. N. R. *J. Phys. D: Appl. Phys.* **1996**, *29*, 3173.

(4) Bianchi, C. L.; Gotti, E.; Toscano, L.; Ragaini, V. *Ultrasonics Sonochem.* **1997**, *4*, 317.

(5) Walter, J.; Shioyama, H. *J. Phys.: Condens. Matter* **1999**, *11*, L21.

(6) Walter, J.; Shioyama, H. *Carbon* **1999**, *37*, 1151.

(7) Walter, J. *Synth. Met.* **1997**, *89*, 39.

(8) Volpin, M. E.; Novikov, Y. N.; Lapkina, N. D.; Kasatochkin, V. I.; Struchkov, Y. T.; Kasakov, M. E.; Stukan, R. A.; Povitskij, V. A.; Karimov, Y. S.; Zvarikina, A. V. *J. Am. Chem. Soc.* **1975**, *97*, 3366.

(9) Walter, J. *Philos. Mag. Lett.* **2000**, *80*, 257.

(10) Walter, J.; Shioyama, H. *J. Phys.: Condens. Matter* **2000**, *12*, 367.

(11) Shuvage, A. T.; Helmer, B. Y.; Lyubenova, T. A.; Kraizman, V. L.; Mirmilstein, A. S.; Kvasheva, L. D.; Novikov, Y. U.; Volpin, M. E. *J. Phys. France* **1989**, *50*, 1145.

(12) Hepel, M. *J. Electrochem. Soc.* **1998**, *145*, 124.

(13) Walter, J. *Adv. Mater.* **2000**, *12*, 31.

(14) Boeck, A.; Rüdorff, W. *Z. Anorg. Allg. Chem.* **1972**, *392*, 236.

(15) Tilquin, J. Y.; Côté, R.; Veilleux, G.; Guay, D.; Dodelet, J. P.; Denés, G. *Carbon* **1995**, *33*, 1265.

(16) Shirai, M.; Igeta, K.; Arai, M. *Chem. Commun.* **2000**, 623.

estimate. Graphite intercalation compounds commonly show an increased electric anisotropy relative to pristine graphite because of a charge transfer between the host and guest. The electrical conductivity parallel to the graphene sheets is enhanced in relation to pristine graphite. However, graphite with embedded nanoparticles are characterized as metal-graphites. This means that there is no longer a charge transfer interaction between the carbon and the embedded metal nanoparticles.<sup>9</sup> Therefore, they are no longer GICs. As far as we know, no electrical conductivity measurements have been carried out on metal-graphite. The only published data until now has been based on GICs.<sup>17</sup> Because of the formation of nanoparticles inside the interlayer space, internal stress occurs inside the carbon lattice. Cracks in the basal plane can often be observed. In such cases the electrical conductivity parallel to the graphene sheets can be less than that in pristine graphite. The electrical conductivity perpendicular to the graphene sheets should be not affected. Because not all layers are occupied by nanoparticles, an appreciable electrical conductivity perpendicular to the graphene sheets is not possible.

Sonochemistry has been established as a powerful tool for chemical synthesis for several years. Colloidal-dispersed platinum has been obtained by sonochemical reactions.<sup>18</sup> The goal for the current study is to establish a new and easy synthesis method to perform intercalation reactions of graphite and to obtain tiny metal particles in the carbon lattice. For the first time a sonochemical approach was used for the intercalation reaction as well as for the reduction of a GIC.

### Experimental Section

**Preparation of a GIC Precursor.** The host material is well-crystalline natural graphite (grade RFL 99.9-S) from Graphitwerke Kropfmühl, Germany. The graphite was mixed in a bottle with  $\text{H}_2\text{PtCl}_6$  and dry thionyl chloride ( $\text{SOCl}_2$ ) from Wako Chemicals, Japan. The bottle was sealed by a cap and then the suspension was sonicated for 3 days in a Yamato 1510J-MT ultrasonic bath (70 W, 42 kHz) at room temperature. No temperature control to the sonobath was applied. Water was used as the filling medium of the bath. The water temperature increased only slightly by sonication.

It should be noted that an attempt to intercalate  $\text{H}_2\text{PtCl}_6$  in the presence of dry  $\text{CCl}_4$  failed. Nanoparticles could be obtained if only thionyl chloride was added to the mixture. By electron microscopy more particles could be observed if a mixture of  $\text{CCl}_4$  and  $\text{SOCl}_2$  was used for oxidation.

For safety reasons plastic bottles should be used. This is because gaseous reaction products appear by sonication, which could burst a bottle. Eyes should be protected by goggles.

Successful intercalation was proven by means of a Rigaku RINT 2000 X-ray powder diffractometer with the following operating conditions: 40 kV, 200 mA, Cu  $\text{K}(\alpha)$  radiation, and step size  $0.02^\circ$ .

**Nanoparticle Preparation.** The GIC was transferred into a cell filled by acetone. Hydrogen gas was flowed through the cell at room temperature while the mixture was sonicated. The suspension was sonicated for 2 days in the same ultrasonic bath. For reasons of safety, all connections between the reaction cell and the hydrogen cylinder should be checked for leaks before the reaction is started.

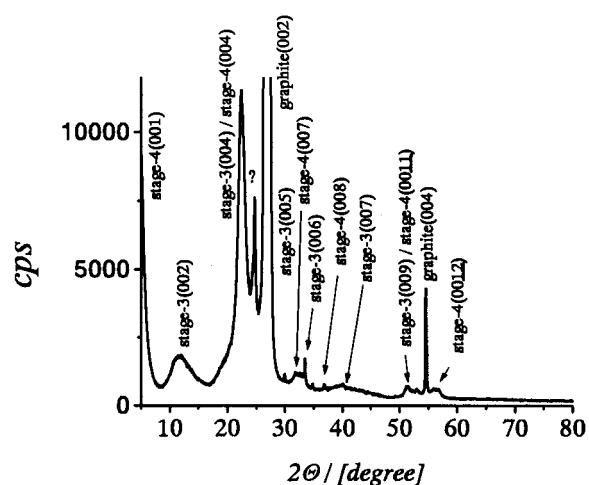


**Figure 1.** XRD pattern of a  $\text{H}_2\text{PtCl}_6$ -GIC precursor, a mixture of a third and fourth stage together with unreacted graphite (see text), can be observed.

It should be mentioned that nanoparticle formation is possible with a reduction time of only a few hours. To get full (no Cl signal by XPS) or nearly complete (small Cl signal by XPS) reduced samples, higher reduction times are required.

The average particle size was estimated by an X-ray powder diffractometer under the same conditions as above. A Hitachi H-800 transmission electron microscope operated at 200 kV was used for bright field images and selected-area electron diffraction (SAED). The camera length was varied and is given in the appropriate figure captions (without refinement). The graphite reflections were used as internal standards and for refinement of the camera constant. X-ray photoelectron spectra (XPS) were collected by a Rigaku DPS 7000 spectrometer having a base pressure better than  $10^{-5}$  Pa. The spectrometer was equipped with an unmonochromized Mg source ( $\text{K}\alpha$  radiation) and operated at 25 kV and 10 mA, the pass energy was 15 eV, and the step size was 0.1 eV. An external silver standard was used (Ag signal at 367.9 eV) to calibrate the energy scale of the spectrometer.

### Results and Discussion

**The Precursor.** A GIC with  $\text{H}_2\text{PtCl}_6$  as a guest was described by Boeck and Rüdorff.<sup>14</sup> These authors gave the identity period in  $c$  direction with 1606 pm for a stage-three compound.<sup>14</sup> A stage-three compound means that every third graphene (IUPAC nomenclature of a single carbon layer with graphitic character) sheet is adjacent to a guest layer. Every third interlayer distance is expanded to 936 pm. All other interlayer distances show the common value of 335 pm. The identity period in the  $c$  direction is one filled layer (936 pm) + two empty layers ( $2 \times 335$  pm) = 1606 pm. The XRD pattern of the  $\text{H}_2\text{PtCl}_6$ -GIC precursor used is shown in Figure 1. The pattern shows features that are common for highly disordered GICs, as mixed sharp and broad lines of (00 $l$ ) reflections in one series, unsymmetric line shapes, unusual intensity ratios, or missing reflections in one series. All these features are common and theoretically and practically described by Hohlwein and Metz, for example.<sup>19</sup> If the pattern is indexed, reflections of a stage three and stage four together with a larger amount of unreacted graphite can be found. The identity period in the  $c$  direction for the third stage was estimated to be  $I_c = 1566 \pm 49$  pm. For the fourth stage, it was  $I_c = 1966 \pm 15$  pm. The third compound present is unreacted graphite with  $I_c = 670$  pm. Graphite

(17) McRae, E.; Andersson, O. E.; Lelaurain, M.; Polo, V.; Sundqvist, B.; Vangelisti, R. *J. Phys. Chem. Solids* **1996**, *57*, 827.

(18) Caruso, R. A.; Ashokkumar, M.; Grieser, F. *Colloids Surf. A*, **2000**, *169*, 219.

(19) Hohlwein, D.; Metz, W. *Z. Kristallogr.* **1974**, *139*, 279.

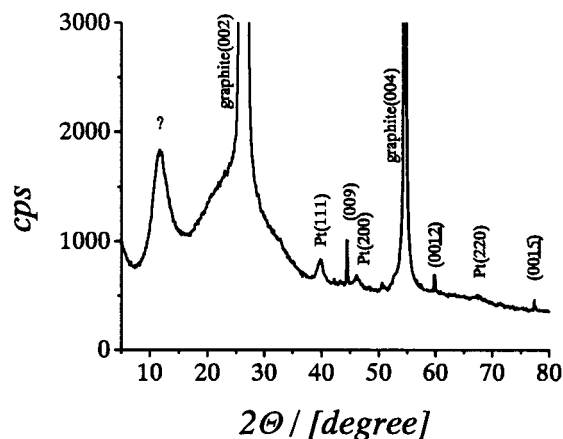


**Figure 2.** XRD pattern after reduction by sonochemistry. The reduction is complete; a new identity period can be estimated (see text). The precursor partly deintercalates after the applied reduction condition.

intercalation compounds are organized in domains, it meaning that the islands are randomly distributed throughout the host lattice. The random occurrence of those three distinguishable identity periods give rise to the observed XRD pattern. The slight misfit between  $I_c = 1566 \pm 49$  pm for a stage three GIC in a disordered compound and  $I_c = 1606$  pm<sup>14</sup> in an ordered GIC (only one stage) can be explained by tiny shifts in the peak positions of (00 $l$ ) reflections (see ref 19). The observed identity period with the standard deviation fits with an ordered sample.

The intercalation by a sonochemical approach was successful, although not all the graphite is intercalated, and a stage mixture is formed. For the formation of a metal chloride GIC, the graphite must be oxidized. Two possible chlorine radical precursors were added:  $\text{CCl}_4$  and  $\text{SOCl}_2$ . A former study by Francony and Pétrier<sup>20</sup> showed that carbon dioxide and activated species as chlorine radicals can be produced by sonofication of  $\text{CCl}_4$ . The excess chlorine will be bonded in the GIC.<sup>7</sup> It should be noted that by sonification a larger amount of gaseous products were formed, which generated a bulb in the plastic cap of the bottle. Upon opening, a large overpressure could be observed.

**Nanoparticle Formation.** After reduction, are the particles if Pt embedded in the interlayer space of graphite? Indeed, the XRD pattern (Figure 2) shows that they are. Partly unreacted graphite can be identified by the graphite (002) reflection observed together with reflections indicating embedded particles. If such reflections are indexed, they show a series of (00 $l$ ) reflections, from which the identity period ( $I_c = 1835 \pm 20$  pm) can be estimated. For calculation of the average particle thickness, we have to subtract the host lattice. The precursor was a mixture of a third and fourth stage. So the average particle thickness is 495 pm, which fits very well with a Pt layer thickness of two Pt atoms (stage four) and with three Pt layers in the case of a third-stage precursor, if the Pt van der Waals diameter is assumed as 278 pm. Tiny reflections for fcc Pt can also be observed. These belong to Pt contaminations at the surface.

A transmission electron microscopic study of the reduced sample showed indeed that the graphite lattice is inhomogeneously intercalated because large areas are

not occupied by nanoparticles, and other regions are densely populated (Figure 3a–c). In some regions an agglomeration of particles can be observed. The corresponding SAED pattern are shown in Figure 3d–f. A region not filled by particles is shown in Figure 3a; the corresponding SAED pattern (Figure 3d) consists only of graphite reflections. The Pt-filled regions (Figure 3b,c) show SAED pattern (Figure 3e,f) that consists of point reflections for the graphite lattice and additional polycrystalline diffraction rings for the embedded particles. If their spacings (see Table 1) are compared to those from the powder diffraction file, it is evident that they are quite distinguishable. The observed SAED pattern can be hexagonally indexed and the  $a$  axis can be calculated as  $427 \pm 12$  pm. This is approximately a ( $2 \times a_{\text{graphite}}$ ) superstructure with regard to graphite ( $a_{\text{graphite}} = 245.4$  pm). The mismatch between the particles and the theoretically expected superstructure is  $\sim 12\%$ . However, nanoparticles show often lattice contraction with regard to the bulk material or an underlying substrate.<sup>21</sup> The degree of lattice contraction depends on the particle size. With decreasing particle size the lattice contraction increases.<sup>22–24</sup> Lattice contraction in nanoparticles appears to be due to the reduction of coordination numbers or to surface bond contractions<sup>22,23</sup> and to a lesser extent by supersaturation of the vacant lattice sites with regard to the bulk.<sup>25</sup> Palladium nanoparticles embedded into graphite with an average lateral dimension of 52 nm show a lattice contraction of approximately 4%.<sup>13</sup> The currently observed nanoparticles are much smaller than the Pd particles, so the mismatch should be larger.

One feature observed only by sonochemical reduction is that the metallic particles tend to agglomerate in some regions, but not in others (Figure 4). The reason for this behavior is unclear and it was not observed by Pt nanoparticles/nanosheets prepared by hydrogen gas reduction in a conventional way.<sup>16</sup>

Why did the particles not show the common fcc reflections? If a fcc lattice is observed by SAED from the [111] direction, it shows a hexagonal diffraction pattern. This is because a crystal is three-dimensional, but a SAED image shows only the diffraction pattern in a plane. If a fcc crystal is observed along the [111] direction by SAED, the diffraction pattern seems to be quasi-hexagonal. The stacking sequence of a fcc unit cell is ABC, if it is observed from the [111] direction. The stacking sequence should be ABCA to obtain fcc reflections. More as one unit cell (trilayer in the stacking sequence ABC) is required to obtain a fcc pattern. As we know from our XRD data, the average particle thickness is two layers. They can never form a fcc unit cell. Metal monolayers in the interlayer space of graphite often mimic the host lattice. Distinguishable, mostly commensurate superstructures with regard to the graphite can be observed, for example, Se-GICs,<sup>10</sup> Ni-GIC,<sup>11</sup> Pd-GIC,<sup>9</sup> or Pd nanoparticles embedded in carbon.<sup>13</sup> If the first layer is resting in a hexagonal arrangement,

(20) Francony, A.; Pétrier, C. *Ultrasonics Sonochem.* **1996**, *3*, S77.

(21) Finch, G. I.; Fordham, S. *Proc. Phys. Soc.* **1936**, *48*, 85.

(22) Goldschmidt, V. M. *Ber. Deut. Chem. Ges.* **1927**, *60*, 1270.

(23) Pauling, L. *J. Am. Chem. Soc.* **1947**, *69*, 542.

(24) Sun, C. Q. *J. Phys.: Condens. Matter* **1999**, *11*, 4801.

(25) Yu, X. F.; Liu, X.; Zhang, K.; Hu, Z. Q. *J. Phys.: Condens. Matter* **1999**, *11*, 937.



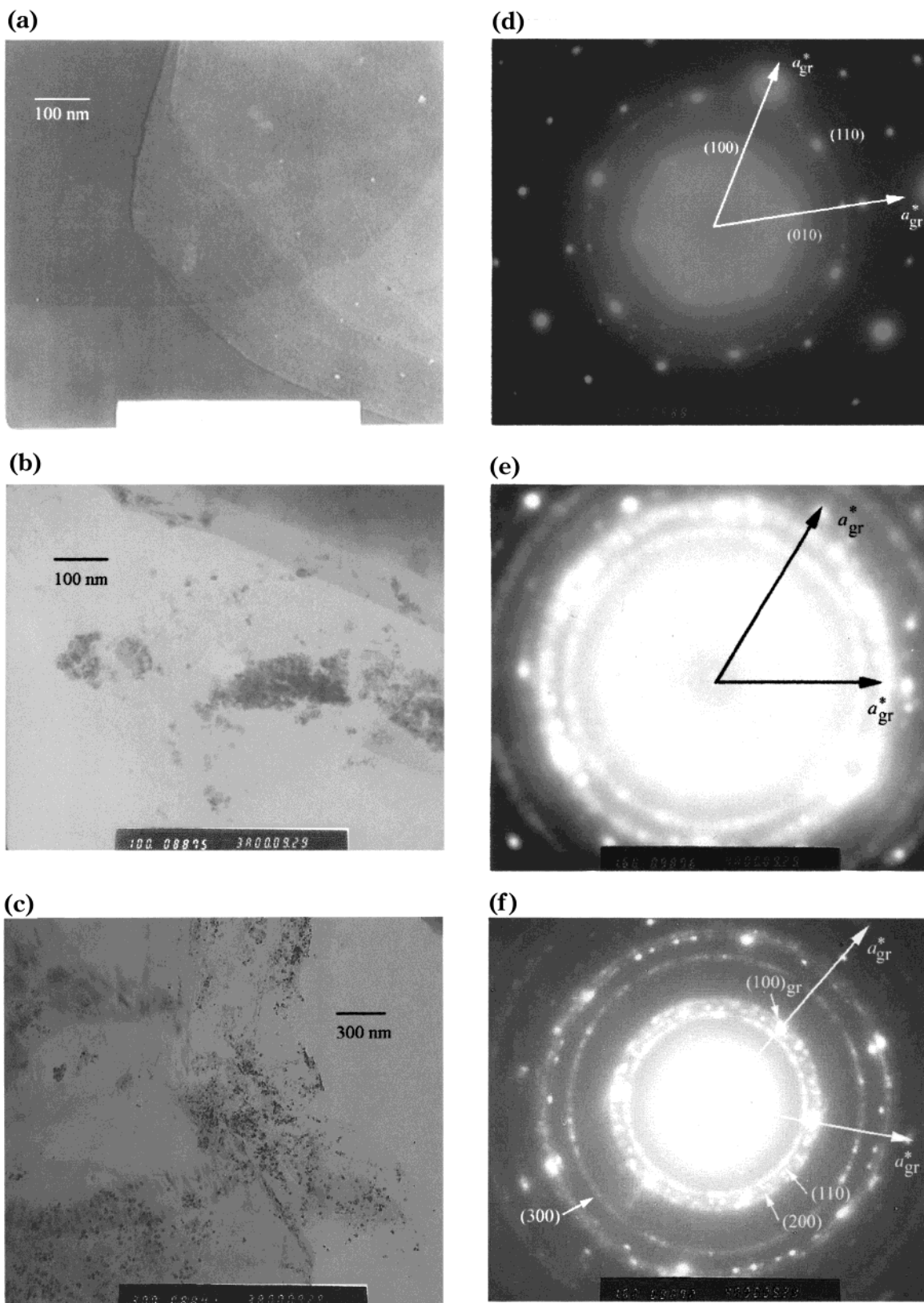


**Figure 3.** (a) A graphite domain, nearly not occupied by particles. (b) Nanoparticles showing some agglomeration, but the particle size is quite small and in a narrow size range (see text). (c) Bright field image of an area occupied by nanoparticles in a narrow size range. (d) SAED pattern from Figure 3a, camera length 1.2 m, "gr" indicates graphite. These few particles give nearly no reflections, but the graphite reflections are easy to observe, "gr" indicates graphite. (e) SAED pattern from Figure 3b, camera length 1.6 m. The point reflections belong to graphite and the polycrystalline diffraction rings to the particles. A ( $2 \times a_{\text{graphite}}$ ) superstructure could be observed (see text). (f) SAED pattern from Figure 3c, camera length 1.6 m, "gr" indicates graphite. All reflections without "gr" as the index belong to Pt. The same superstructure could be observed.

atoms have the highest possible symmetry and they are templated by the carbon lattice. In such a case the

second layer should rest in a stacking sequence AB with hexagonal symmetry. In the case of Pd particles encap-

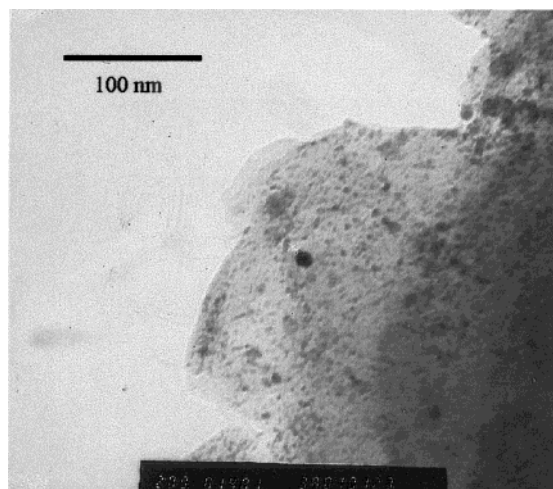


**Figure 4.** TEM bright field image of an area with mostly tiny Pt particles in the size range 1–10 nm; some larger particles can also be seen. These particles are definitely smaller than those by Shirai et al. [16], who used conventional reduction.

**Table 1. Experimentally Observed  $d$  Spacings by SAED, Indexed as Hexagonal (for Convenience Observed Graphite Reflections Are Not Listed), and Pt Reflections and Indexing (fcc) Taken from the Powder Diffraction File<sup>33</sup>**

$d_{\text{hex}}$ (pm)	$hkl$	$d_{\text{fcc}}$ (pm)	$hkl$
236.6	110	226.5	111
217.9	200	196.2	200
144.0	300	138.7	220
123.6		118.3	311
118.3		113.3	222
107.5	400	98.1	400
94.1		90.0	331
82.0	500	87.7	420
		80.1	422

sulated into graphite<sup>26</sup> two distinguishable superstructures can be observed. They are ( $2 \times a_{\text{graphite}}$ ) and ( $3 \times a_{\text{graphite}}$ ) superstructures,<sup>13</sup> which are due to different self-organizations in the carbon lattice. It should be noted that the SAED pattern of Pd multilayer nanoparticles can often be indexed with mixed hcp and fcc reflections. On the other hand, if Al or Au is deposited on a graphite surface in thicknesses of two layers, also hexagonal particles with a ( $2 \times a_{\text{graphite}}$ ) superstructure ( $a = 424$  pm) can be observed.<sup>27</sup> The graphite lattice was not affected by the sonochemical treatment.

Another interesting observation is that not all reflections can be indexed; see Table 1. This can be explained by the restricted dimension of the particles. The selection rules fit always with three-dimensional crystals. A very interesting experiment was done by Finch and Wilman<sup>28</sup> and they observed for a graphite slab by SAED that all reflections were in order with the selection rules. Then, they started to thin the same slice and observed it again. At first, all patterns showed reflection in accordance with the selection rules. As the slice came into the range of a few layers in thickness, they observed several reflections that were forbidden in the bulk and before (as the same slice was thicker) never been observed by SAED. They concluded<sup>28</sup> that the occurrence of forbidden reflections in the SAED

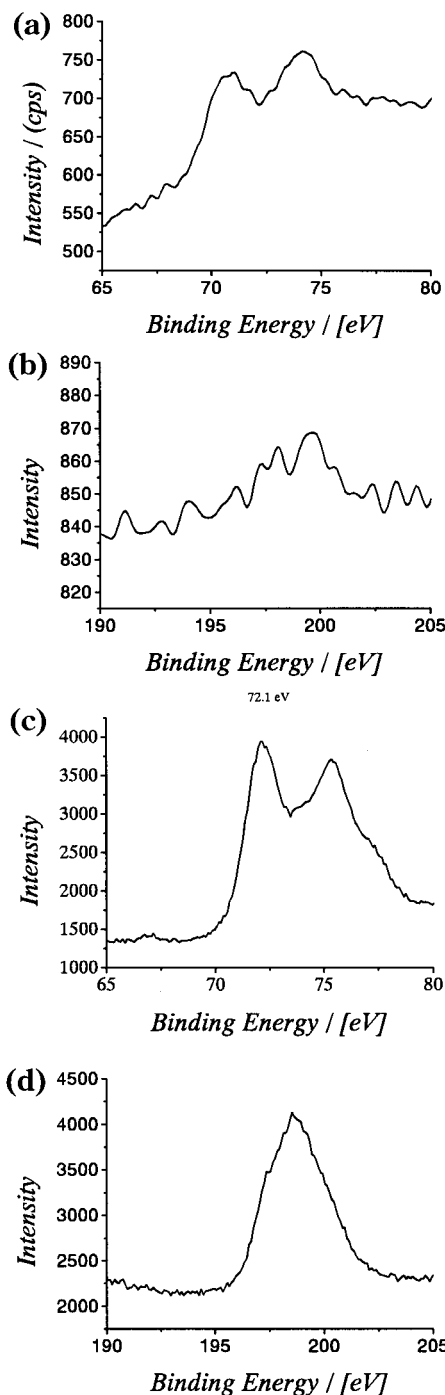


**Figure 5.** (a) The Pt core level spectrum, ( $4f_{7/2}$ ) at 70.8 eV. This is contributed to metallic platinum. (b) The Cl core level spectrum. A signal is not detectable. (c) For comparison the Pt core level spectrum of the precursor. After deconvolution two signals can be measured; they show nonmetallic states. (d) For comparison, the Cl core level spectrum of the precursor. A well-pronounced signal at 198.5 eV is detectable.

pattern of ultrathin slabs was due to the limited dimension of the crystal. The unindexed reflections in Table 1 were compared to the  $\text{H}_2\text{PtCl}_6$ -GIC precursor, but they did not coincide.

If the spacings of the particles are not identical to the powder diffraction file data and we claim that they are due to Pt metal, we should confirm this by X-ray photoelectron spectroscopy (XPS). The core level spectra of Pt and Cl were measured for the precursor as well as for the reduced sample.

(26) Walter, J.; Shioyama, H. *Phys. Lett. A* **1999**, *254*, 65.

(27) Endo, T.; Sumomogi, H.; Maeta, H.; Ohara, S.; Fujita, H. *Materials Trans., JIM* **1999**, *40*, 903.

(28) Finch, G. I.; Wilman, H. *Proc. R. Soc. A* **1936**, *155*, 345.

The graphite flakes containing nanoparticles show a Pt core level spectrum with a signal ( $\text{Pt}_{4f_{1/2}}$ ) at 70.8 eV (Figure 5a). This is definitely platinum in a metallic state ( $\text{Pt}^0$ ). The chlorine core level spectrum shows only a rough baseline (Figure 5b). It can be concluded that the  $\text{H}_2\text{PtCl}_6$  precursor is reduced by hydrogen gas, HCl is formed and escaped from the host lattice, and metallic Pt particles remained inside the carbon. For comparison Figure 5c,d shows the core level spectra of Pt and Cl for the precursor. The Pt signal is shifted to 72.1 eV. If the signal is deconvoluted, two doublets can be observed: with  $\text{Pt}_{4f_{1/2}}$  at 73.0 and 74.8 eV, respectively. A pronounced Cl core level signal at 198.5 eV could be obtained (Figure 5d). The XPS spectra of the precursor and of the reduced sample are very distinguishable and demonstrate that the reduction was complete. The observed shift at 70.8 eV for the reduced sample indicates the presence of metallic Pt.

### Conclusion

The intercalation of a metal chloride into a graphite host lattice by a sonochemical approach was successful. The lattice is not fully intercalated, but this often

happens by conventional techniques too. Reduction of a GIC can be carried by sonochemistry. This opens a new, inexpensive, and easy way to produce graphite intercalation compounds as well as nanoparticles inside graphite. The graphite lattice was not affected by the sonochemical treatment. Particles observed in the interlayer space are bilayers or trilayers. Therefore, they cannot crystallize in a fcc lattice (bilayers) as is common for the metal in the bulk nor can they show a SAED pattern with full fcc symmetry (trilayers). Physical properties often change with crystal symmetry, for example, bulk Ta crystallizes only in bcc,<sup>29</sup> but thin films can be fcc<sup>30,31</sup> or tetragonal<sup>29</sup> and they show different physical properties.<sup>29</sup> The main advantage of the sonochemical approach is maybe that the process leads to relatively tiny Pt nanoparticles inside the graphite lattice, which are much smaller than Pd<sup>26</sup> or Pt<sup>16</sup> nanoparticles encapsulated into graphite produced by a conventional gas-phase reaction. This could be interesting for catalysis. Pd nanoparticles (average size 52 nm in lateral direction) encapsulated into graphite have been shown to be active catalysts for the Heck reaction.<sup>32</sup>

**Acknowledgment.** The authors acknowledge financial support from the Ministry of Cultural Affairs, Education and Sport, Japan, under the grant for young scientists no. 70314375.

CM000898R

(29) Read, M. H.; Altman, C. *Appl. Phys. Lett.* **1965**, *7*, 51.

(30) Denbigh, P. N.; Marcus, R. B. *J. Appl. Phys.* **1966**, *37*, 4325.

(31) Chopra, K. L.; Randlett, M. R.; Duff, R. H. *Philos. Mag.* **1967**, *16*, 261.

(32) Walter, J.; Heiermann, J.; Dyker, G.; Hara, S.; Shioyama, H. *J. Catal.* **2000**, *189*, 449.

(33) Powder diffraction file 4-0802, Pt metal.